ORGANOMETALLICS

Article

pubs.acs.org/Organometallics

Chiral Iron(II) NPPN Complexes: Synthesis and Application in the Asymmetric Strecker Reaction of Azomethine Imines

Raffael Huber, Raphael Bigler, and Antonio Mezzetti*

Department of Chemistry and Applied Biosciences, ETH Zürich, CH-8093 Zürich, Switzerland

Supporting Information

ABSTRACT: The open-chain NPPN ligand (1*S*,1′*S*)-1,1′-((ethane-1,2-diylbis(phenylphosphanediyl))bis(2,1-phenylene))bis(*N*-cyclohexylmethanimine) (**1**) was prepared by condensation of cyclohexylamine with enantiomerically pure (1*S*,1′*S*)-2,2′-(ethane-1,2-diylbis(phenylphosphanediyl))dibenzaldehyde ((*S*,*S*)-**6**). Ligand **1** coordinates to $[Fe(OH_2)_6](BF_4)_2$ or $[Fe(MeCN)_6](SbF_6)_2$ in acetonitrile to give the dicationic complex $[Fe(MeCN)_2(\mathbf{1})](X)_2$ (**2**) (X = BF_4^- or SbF_6^-). The corresponding carbonyl (**3**), bromocarbonyl (**4**), and bis(*tert*-butylisonitrile) (**5**) derivatives were prepared and fully characterized. Complex **2** reacts with Me_3SiCN to give the corresponding trimethylsilyl isocyanide derivative **18** featuring a Fe−$CNSiMe_3$ linkage. The X-ray structures of **2**, **3**, **5**, and **18** show that ligand **1** assumes the Λ-*cis*-α geometry, which allows comparing the *trans* influence of these ligands. Complexes **2**, **3**, **5**, and **18** were applied in the asymmetric addition of trimethylsilyl cyanide to azomethine imines (Strecker reaction), whose enantioselectivity reached 22% ee. The low enantioselectivity can be explained on the basis of the Me_3SiCN/Me_3SiNC isomerization and of the reaction product partially displacing the NPPN ligand from iron.

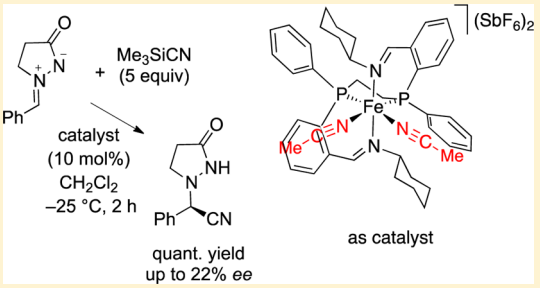

INTRODUCTION

Being able to replace precious metals with iron provides several advantages: iron is cheap, nontoxic, and environmentally benign. Catalysts based on iron are employed for a broad range of transformations,[1] and nature uses it for some of the most challenging reactions, such as the direct C−H oxidation of methane.[2] There are, however, serious obstacles that have to be overcome in order to successfully use iron—and base metals, in general—in catalysis. In particular, 3d metals give weaker metal−ligand bonds, which often results in high-spin electron configurations. The resulting paramagnetic species not only elude characterization by traditional NMR experiments but also are less stable than their low-spin counterparts because of the partial occupation of σ*-antibonding orbitals (e_g orbitals in the case of octahedral complexes).

A common approach to tackle these problems is to exploit the chelate effect by using pincer[3] or tetradentate[4] ligands. Strong-field ligands such as CO, isonitriles, or hydrides are also often applied to enforce the low-spin electron configuration. Furthermore, the macrocyclic effect[5] uses ligand preorganization and rigidity to provide a pocket of appropriate size for the metal and to increase the kinetic inertness of the ligand framework, which can be exploited to build robust systems. Accordingly, iron−porphyrin systems are abundant in nature as the active site of enzymes and are widely used.[2]

We recently capitalized on the macrocyclic effect with iron complexes of tetradentate N_2P_2-macrocycles,[6] whereas Gao has successfully applied N_4P_2 macrocycles in asymmetric hydrogenation of ketones with iron.[7] Notably, the diphosphine (*S*,*S*)-**6** that we developed to prepare C_2-symmetric macrocycles is a new, *P*-stereogenic synthon that gives access also to diastereo- and enantiomerically pure open-chain NPPN ligands such as **1** (Scheme 1).

An advantage of Fe/NPPN over Fe/PNNP systems is that the terminal donor is an N atom, which better matches the hardness[8] of Fe^{2+} as compared to the soft PPh_2 terminus of the

Scheme 1. Synthesis of Ligand 1 and Complexes 2

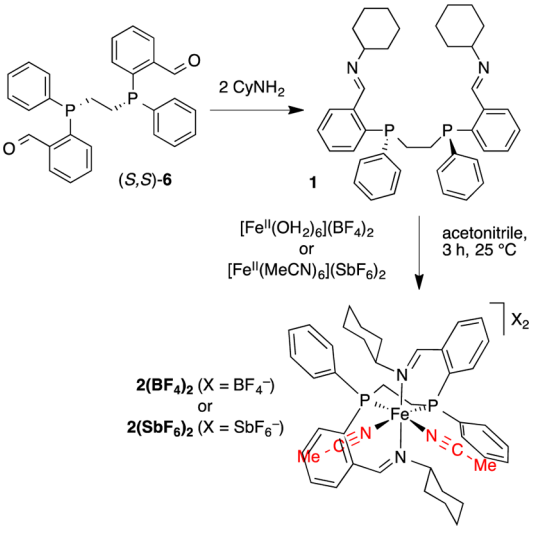

Received: April 28, 2015

DOI: 10.1021/acs.organomet.5b00357
Organometallics XXXX, XXX, XXX−XXX

PNNP ligands. Also, the bulkiness at the terminal donor is lesser in the NPPN ligand **1** than in PNNP. Both factors are expected to increase the stability of NPPN complexes as compared to their PNNP analogues, which tend to decompose to iron nanoparticles under harsh reaction conditions.[4t] The present paper describes the synthesis of stable, diamagnetic iron(II) complexes of the type $[Fe(L)_2(NPPN)]^{2+}$ (L = RCN (Scheme 1), CO, or RNC) and a first application in asymmetric catalysis.

Following our experience with Ru/PNNP systems,[9] we initially investigated the potential of Fe/NPPN complexes as Lewis acids. Surprisingly, though, substrate coordination experiments revealed that these iron(II) complexes are highly azaphilic rather than oxophilic. This finding prompted us to study the reactions of azomethine imines, in particular *N,N′*-cyclic ones, which are mainly known for their rich cycloaddition chemistry.[10] Overall, very few examples of nucleophilic addition to azomethine imines are known,[11] of which only two[11d,f] are metal-catalyzed. Inspired by a recent report of a Strecker-type addition of cyanide onto azomethine imines catalyzed by a cinchona-derived hydrogen-bonding catalyst,[12] we here report preliminary results concerning Fe/NPPN-catalyzed cyanide addition onto 2-benzylidene-5-oxopyrazolidin-2-ium-1-ide.

RESULTS AND DISCUSSION

Λ-*cis*-α-$[Fe(MeCN)_2(1)]^{2+}$ (2). Condensation of enantiomerically pure (1*S*,1′*S*)-2,2′-(ethane-1,2-diylbis(phenylphosphanediyl))dibenzaldehyde ((*S,S*)-**6**)[6a] with cyclohexylamine gave the new open-chain NPPN ligand **1** (Scheme 1). Hexaaquairon(II) tetrafluoroborate or hexakis(acetonitrile)-iron(II) hexafluoroantimonate[13] react with **1** in acetonitrile at room temperature to give the corresponding stable, diamagnetic iron(II) complexes $[Fe(MeCN)_2(\mathbf{1})](BF_4)_2$ (**2**$(BF_4)_2$) and $[Fe(MeCN)_2(\mathbf{1})](SbF_6)_2$ (**2**$(SbF_6)_2$), respectively. The hexafluoroantimonate salt gives better elemental analyses as compared to the tetrafluoroborate derivative, whose carbon values are generally too low, probably due to combustion problems.[14]

The complexation of **1** to Fe(II), which is accompanied by a color change of the reaction solution from colorless to red, reaches completion within 3 h, as indicated by the disappearance of the $^{31}P\{^1H\}$ NMR signal of free **1** at δ −25.2. The new singlet at δ 88.3 is assigned to *cis*-α-**2** (98%) and the low-intensity (2%) singlet at δ 93.0 to a different isomer of **2** (possibly the *trans* one). The high chemical shift of **2** as compared to Fe/PNNP complexes,[4n] which resonate around δ 50, is a first indication of a strong chelate effect.[15] The ^1H NMR signal of the equivalent imine H atoms (*H*C═N) is a singlet, and a P,H correlation experiment showed no cross peaks between them and the phosphines, which further supports a *cis*-α structure for the main isomer.[16]

Complex **2**$(BF_4)_2$ was studied by X-ray diffraction. Crystals of **2**$(BF_4)_2$ were grown from CH_2Cl_2/Et_2O. The Fe atom lies on a two-fold axis, and the complex adopts the Λ-*cis*-α structure (Figure 1), in contrast to Ru/PNNP[9] or Fe/PNNP systems,[4n] which usually adopt the *trans* structure. The pseudo-octahedral geometry is slightly distorted, as the N(1)−Fe−N(2) angle is acute (84.85(9)°) due to steric repulsion between the cyclohexyl group on N(1A) and the MeCN ligand containing N(2) (Table 1). The Fe−P bond distance is shorter in the NPPN derivative **2** than in the PNNP complex *trans*-$[Fe(MeCN)_2((R,R)$-$\{PPh_2(o\text{-}C_6H_4)CH{=}NC_6H_{10}N{=}CH(o\text{-}C_6H_4)PPh_2\})]$ (2.2161(6) vs 2.276(2)/2.272(2) Å, respectively),[4n] whereas the imine−iron bond is longer (2.028(2) vs 2.007(6)/2.010(6) Å). We suggest that this reflects the effect of the different chelate in the NPPN and PNNP complexes, which strengthens the Fe−P bond in the former and the Fe−imino ligation in the latter. The Fe−NCMe bond in **2** (1.976(2) Å) is about 6 pm longer than in Fe/PNNP (1.915(7)/1.904(4) Å), which originates from the higher *trans* influence of phosphine as compared to acetonitrile. This may lead to a more labile acetonitrile ligand, which should facilitate ancillary ligand exchange.

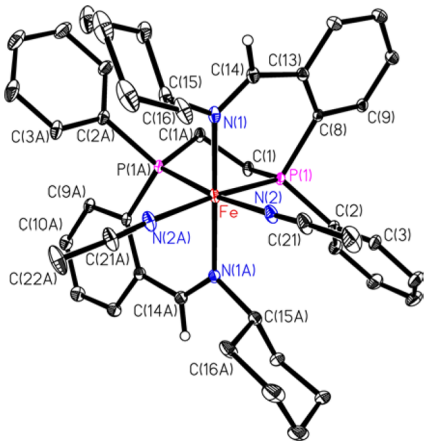

Figure 1. ORTEP drawing of the complex cation of **2** (with ellipsoids at 30% probability).

The helical *cis*-α configuration of **2** renders the complex C_2-symmetric and reduces the number of possible diastereoisomers of the catalyst−substrate adduct. This makes **2** a promising candidate for binding bidentate substrates (*vide infra*, Table 4). In fact, a strikingly high number of C_2-symmetric ligands and their metal complexes have proven to be excellent catalysts for enantioselective transformations in the past.[17]

Λ-*cis*-α-$[Fe(CO)_2(1)](BF_4)_2$ (3). The bis(acetonitrile) complex **2**$(BF_4)_2$ reacts with CO (2.25 bar) in acetone to give the dicarbonyl analogue $[Fe(CO)_2(\mathbf{1})](BF_4)_2$ (**3**) (Scheme 2). The reaction is accompanied by a color change from red to yellow. However, acetonitrile must be removed to drive the reaction to completion by evaporating the solution to dryness several times. If not, a mixture of **3** and $[Fe(CO)(MeCN)(\mathbf{1})]^{2+}$ is obtained. A $^{31}P\{^1H\}$ NMR singlet at δ 79.6 confirms that the C_2-symmetric structure is retained in solution. Complex **3** shows ν(CO) bands at 2072 and 2028 cm^{-1}, in the range observed for dicationic dicarbonyl complexes[18] (2094 and 2038 cm^{-1} for $[Fe(CO)_2(N_2P_2)]^{2+}$;[18a] 2059 and 2022 cm^{-1} for $[Fe(CO)_2(P_4)]^{2+}$).[18b] Compared with dicationic monocarbonyl iron(II) complexes such as $[Fe(CO)(MeCN)(PNNP)]^{2+}$ (ν = 2002 cm^{-1}),[19] the wavenumbers are higher and point to a weaker $d_{Fe}{\rightarrow}\pi^*_{CO}$ backdonation, as expected for dicarbonyl derivatives, in which the strong π-accepting CO ligands compete for the electron density of the iron(II) ion.

X-ray-quality crystals of **3** were grown by layering a CH_2Cl_2 solution with Et_2O under CO atmosphere. Similarly to the bis(acetonitrile) complex **2**$(BF_4)_2$, the dicarbonyl derivative **3** crystallizes as the Λ-*cis*-α isomer with the Fe atom on a two-fold axis (Figure 2). The slight distortions from the octahedral geometry found in the bis(acetonitrile) analogue **2**$(BF_4)_2$ are retained in **3** (Table 2).

The Fe−CO bond length in **3** (1.831(4) Å) is in the range observed for *trans* P−Fe−CO moieties in dicarbonyl iron(II)

DOI: 10.1021/acs.organomet.5b00357
Organometallics XXXX, XXX, XXX−XXX

Table 1. Selected Bond Lengths (Å) and Angles (deg) for $2(BF_4)_2$

Fe–P(1)	2.2161(6)	Fe–N(1)	2.028(2)
Fe–N(2)	1.9757(18)	N(2)–C(21)	1.142(3)
Fe–N(2)–C(21)	176.8(3)	N(2)–C(21)–C(22)	176.8(4)
P(1)–Fe–N(1)	94.45(5)	P(1)–Fe–N(1A)	88.45(5)
P(1)–Fe–N(2)	93.15(6)	P(1)–Fe–N(2A)	172.91(7)
N(1)–Fe–N(2)	84.85(9)	N(1)–Fe–N(2A)	92.35(8)
P(1)–Fe–P(1A)	85.04(3)	N(1)–Fe–N(1A)	176.07(11)
N(2)–Fe–N(2A)	89.46(11)		

Scheme 2. Synthesis of Dicarbonyl Complex 3

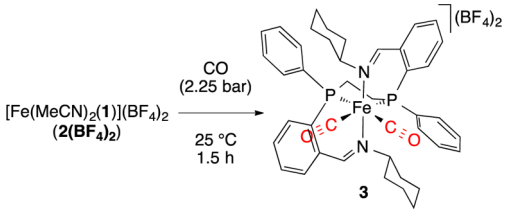

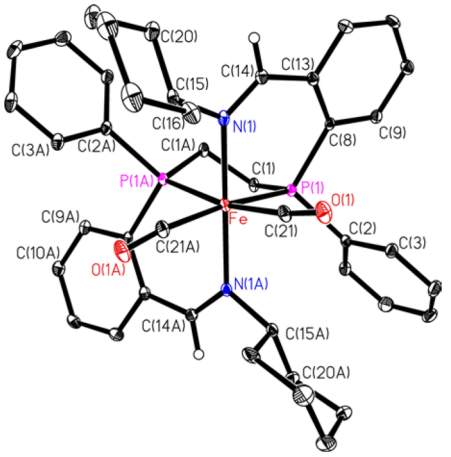

Figure 2. ORTEP drawing of the complex cation of **3** (with ellipsoids at 30% probability).

complexes,[18] such as in *cis*-$[Fe(CO)_2(P_4)]^{2+}$ (1.804(2) and 1.824(3) Å; P_4 = tetradentate phosphine ligand).[18b] Interestingly, *all cis*-$[Fe(CO)_2(P{-}N)_2]^{2+}$ (P–N = chelating P,N ligand) exhibits a long Fe–CO distance *trans* to P (1.837(2) Å) and a short one (1.788(3) Å) *trans* to N.[18a] Unsurprisingly, phosphine has here a larger *trans* influence than nitrogen, which may be relevant to catalysis as the weaker Fe–CO bond may lead to easy dissociation to a reactive 16-electron complex. The weak coordination of CO is in agreement with the fact that MeCN has to be removed several times during the synthesis, which implies that it competes effectively with CO.

[FeBr(CO)(1)](BPh$_4$) (4). The bis(acetonitrile) complex $2(BF_4)_2$ reacts with KBr (2 equiv) under CO (2.25 bar) to give the bromocarbonyl complex **4**, which was isolated as the tetraphenylborate salt as an orange powder (Scheme 3).

Scheme 3. Synthesis of Bromocarbonyl Complex 4

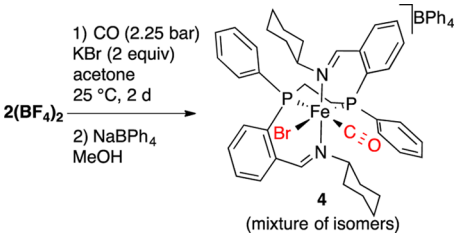

The $^{31}P\{^1H\}$ NMR spectrum (Figure 3) indicates that **4** is formed as a mixture of three isomers **A**, **B**, and **C** in an approximately 3:4:1 ratio (Figure 4). The amount of **A** increases over time (Supporting Information, Figure S11). However, heating the complex to accelerate the thermodynamic equilibration led to the formation of dicarbonyl complex **3** (identified by its $^{31}P\{^1H\}$ NMR chemical shift) and other unidentified species.

The $^{31}P\{^1H\}$ NMR signals were assigned on the basis of the *trans* influence of the ligands. The AX system at δ 93.7 and 68.5 (*trans* to bromo and carbonyl, respectively; $^2J_{P,P'}$ = 49.8 Hz) is assigned to the *cis*-α isomer **4A** (*OC*-6-24). The $^{31}P\{^1H\}$NMR resonances at δ 85.0 (*trans* to imine) and 73.7 (*trans* to carbonyl; $^2J_{P,P'}$ = 38.0 Hz) are diagnostic of structure **B** (*OC*-6-34-*A*). Finally, the signals at δ 91.7 (*trans* to bromo) and 86.9 (*trans* to imine; $^2J_{P,P'}$ = 35.0 Hz) were assigned to the *cis*-β isomer **4C** (*OC*-6-23-*A*). The IR spectrum of **4** displays two carbonyl absorptions at ν = 1986 and 1961 cm^{-1}. Thus, the C–O bond is weaker than in dicarbonyl complex **3**, which reflects the stronger π-backbonding in the monocationic monocarbonyl **4** than in the dicationic dicarbonyl species **3**.

Λ-*cis*-α-[Fe(CN^{t}Bu)$_2$(1)](BF$_4$)$_2$ (5). The bis(acetonitrile) complex $2(BF_4)_2$ reacts with *tert*-butylisonitrile in dichloromethane at room temperature to give Λ-*cis*-α-$[Fe(CN^tBu)_2$-

Table 2. Selected Bond Lengths (Å) and Angles (deg) for 3

Fe–P(1)	2.266(1)	Fe–N(1)	2.020(3)
Fe–C(21)	1.831(4)	C(21)–O(1)	1.139(4)
P(1)–Fe–N(1)	94.36(8)	P(1)–Fe–N(1A)	86.84(8)
P(1)–Fe–C(21)	91.03(11)	P(1)–Fe–C(21A)	169.63(12)
N(1)–Fe–C(21)	84.15(14)	N(1)–Fe–C(21A)	94.75(14)
P(1)–Fe–P(1A)	84.54(5)	N(1)–Fe–N(1A)	178.39(17)
C(21)–Fe–C(21A)	94.8(2)	Fe–C(21)–O(1)	172.4(3)

DOI: 10.1021/acs.organomet.5b00357
Organometallics XXXX, XXX, XXX–XXX

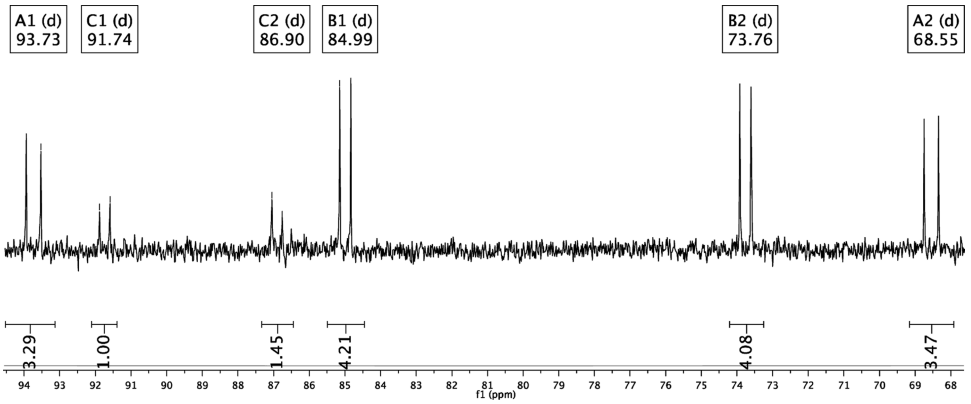

Figure 3. Section of the $^{31}P\{^{1}H\}$ NMR spectrum of bromocarbonyl complex **4**.

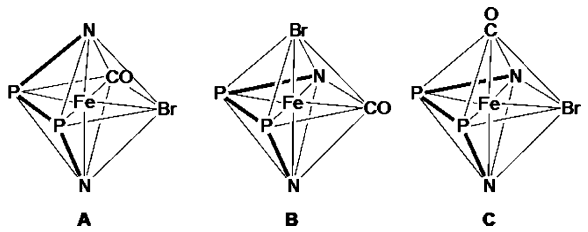

Figure 4. Depiction of the isomers observed by $^{31}P\{^{1}H\}$ NMR spectroscopy for **4**. Ligand **1** is drawn as N−P−P−N.

(**1**)](BF$_4$)$_2$ (**5**) (Scheme 4). The reaction is accompanied by a color change from red to orange. A singlet at δ 82.4 in the

Scheme 4. Synthesis of Bis(isonitrile) Complex 5

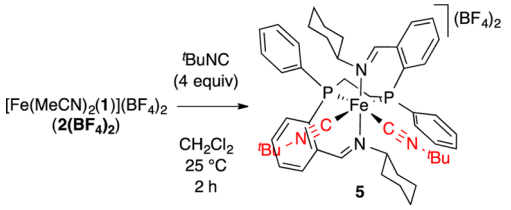

$^{31}P\{^{1}H\}$ NMR spectrum indicates that the complex is C_2-symmetric. On the basis of its electronic similarity to its dicarbonyl analogue **3**, a *cis-α* structure can be assumed. This hypothesis is further supported by the presence of two bands for the isonitrile NC stretching at 2162 and 2143 cm^{-1} in the IR spectrum.

An X-ray study of crystals grown from CH_2Cl_2/Et_2O confirmed the structural assignment. The NPPN ligand adopts the Λ-*cis-α* configuration with the Fe atom on a crystallographic two-fold axis (Figure 5). The Fe−CN^{t}Bu bond distance (1.896(3) Å, Table 3) is just ca. 7 pm longer than the Fe−CO separation in **3** (1.831(4) Å), which confirms the similarity of the CO and NCR ligands and the possible use of isonitriles as "tunable carbonyls".[6b,c] The P(1)−Fe−C(21) angle is slightly enlarged from 91.03(11)° in **3** to 94.80(9)° in **5**, in agreement with *tert*-butylisonitrile being considerably more bulky than acetonitrile or carbon monoxide.

X-ray structures of dicationic Fe(II) isonitrile complexes containing both P and N donors are extremely rare.[6,20] We have recently reported N_2P_2 macrocyclic complexes of iron(II) of the type $[Fe(CNR)_2(N_2P_2)]^{2+}$.[6] The Fe−CN^{t}Bu bond distances *trans* to P are indistinguishable (1.896(3) and 1.8856(17) Å in **5** and in the latter complex). In contrast,

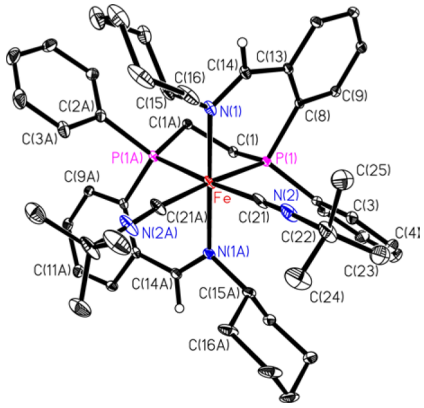

Figure 5. ORTEP drawing of the complex cation of **5** (with ellipsoids at 30% probability).

the Fe−C distance *trans* to imino in the macrocycle derivative is significantly shorter (1.8433(17) Å), which reflects a lower *trans* influence of imine as compared to phosphine. A similar trend is observed in the Fe−C bond length in [Fe(PNP)-(CN^{t}Bu)$_3$](BF$_4$)$_2$ (1.854(2) Å (*trans* to N); 1.889(2) and 1.881(2) Å (*trans* to isonitrile)).[20]

As complexes **2**, **3**, and **5** exhibit very similar geometries (Supporting Information, Table S1), the comparison of Fe−P bond lengths gives insight into the relative *trans* influence[21] of acetonitrile, carbon monoxide, and *tert*-butylisonitrile. The shortest Fe−P bond is found in the bis(acetonitrile) adduct **2** (2.2159(5) Å) and the longest one in the dicarbonyl complex **3** (2.2663(11) Å), with the ones in isonitrile complex **5** lying in between (2.2458(7) Å). Hence, for such systems, the carbonyl ligand has the strongest *trans* influence, followed by *tert*-butylisonitrile and eventually acetonitrile. Little is known about the *trans* influence of isonitriles[22] and, to the best of our knowledge, this is its first assessment in iron complexes containing at least one phosphine donor.

Reactivity of [Fe(MeCN)$_2$(1)]$^{2+}$ (2). Preliminary tests of the Fe/NPPN complexes in the asymmetric transfer hydrogenation of ketones were not promising. The bis(acetonitrile) derivative **2** was inactive and decomposed under reaction conditions as already observed for analogous Fe(MeCN)$_2$ complexes,[4t,6b,c] whereas the CN^{t}Bu analogue **5** gave low enantioselectivity (21% ee, see Supporting Information).

As an alternative, we investigated the potential of Fe/NPPN complexes as Lewis acids. Several substrates containing oxygen and/or nitrogen functionalities (such as carbonyl or imine)

DOI: 10.1021/acs.organomet.5b00357
Organometallics XXXX, XXX, XXX−XXX

Table 3. Selected Bond Lengths (Å) and Angles (deg) for 5

Fe–P(1)	2.2458(7)	Fe–N(1)	2.054(2)
Fe–C(21)	1.896(3)	C(21)–N(2)	1.157(4)
Fe–C(21)–N(2)	173.5(3)	C(21)–N(2)–C(22)	177.2(3)
P(1)–Fe–N(1)	92.09(6)	P(1)–Fe–N(1A)	88.73(7)
P(1)–Fe–C(21)	94.80(9)	P(1)–Fe–C(21A)	175.4(1)
N(1)–Fe–C(21)	86.70(12)	N(1)–Fe–C(21A)	92.47(12)
P(1)–Fe–P(1A)	85.64(4)	N(1)–Fe–N(1A)	178.88(13)
C(21)–Fe–C(21A)	85.13(17)		

were studied to explore the reactivity of the bis(acetonitrile) complex **2** (Chart 1). In each case, the appropriate substrate

Chart 1. Coordination Experiments with $2(BF_4)_2$[a]

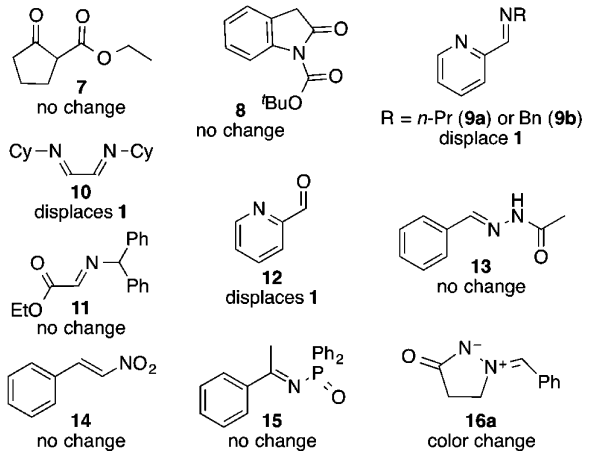

[a]Complex $2(BF_4)_2$ (5 mg, 5.4 μmol) was dissolved in CD_2Cl_2 (0.5 mL). The substrate (54 μmol, 10 equiv) was added, the mixture was shaken for 30 min, and the $^{31}P\{^1H\}$ NMR spectrum of the solution was recorded.

and $2(BF_4)_2$ were mixed in a 10:1 molar ratio in CD_2Cl_2 at room temperature, and the reaction was monitored by $^{31}P\{^1H\}$ NMR spectroscopy. Based on our experience with dicationic Ru/PNNP complexes, which give stable *O,O*-chelate complexes with 1,3-dicarbonyl compounds,[9a−d] we tested ethyl 2-oxocyclopentane-1-carboxylate (**7**) and *tert*-butyl 2-oxoindoline-1-carboxylate (**8**) first. However, neither **7** nor **8** reacted with $2(BF_4)_2$ (Chart 1). In contrast, chelating diimines such as *N*-alkyl-1-(pyridin-2-yl)methanimine (**9**) or N^1,N^2-dicyclohexylethane-1,2-diimine (**10**) displaced the NPPN ligand **1** from $2(BF_4)_2$. Their reaction with $2(BF_4)_2$ was instantaneous, as indicated by the color change of the reaction solution, and was confirmed by its $^{31}P\{^1H\}$ NMR spectra, in which the only signal was that of the free ligand **1** at δ −25.2. Although diimines are good ligands,[23] the outcome of the reaction was nonetheless surprising, as the multiple chelate effect of the tetradentate ligand **1** should give robust complexes.

Therefore, we tried to fine-tune the donor properties of the substrate by using α-iminoester **11**, *o*-formylpyridine **12**, acylhydrazone **13**, nitrostyrene **14**, phosphinoylimine **15**, and azomethine imine **16a**. All these substrates either did not coordinate or displaced the NPPN ligand **1** from the iron(II) ion. Interestingly though, azomethine imine **16a** gave an instantaneous color change from light to deep red upon addition. As no change was observed in the $^{31}P\{^1H\}$ NMR spectrum, we speculate that a weak interaction takes place between **2** and **16a**. This observation prompted us to test complexes **2**−**5** as Lewis acids in catalytic reactions of azomethine imines.

Asymmetric Strecker-Type Addition to Azomethine Imines. In preliminary experiments with 2-benzylidene-5-oxopyrazolidin-2-ium-1-ide (**16a**), acrylonitrile was tested as 1,3-dipolarophile, and trifluoromethyltrimethylsilane, allyltrimethylsilane, and trimethylsilyl cyanide as nucleophiles. In these experiments, only Me_3SiCN reacted with azomethine imine **16a** in the presence of the chiral Lewis acid $2(BF_4)_2$ under the conditions given in Scheme 5. As 2-(3-oxopyrazolidin-1-yl)-2-

Scheme 5. Asymmetric Strecker Reaction

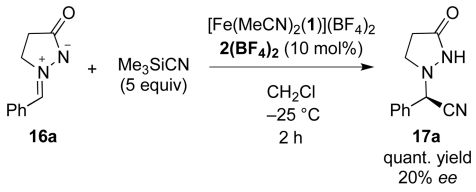

phenylacetonitrile (**17a**) was formed with low, but significant enantioselectivity (20% ee), we focused our attention on cyanide addition onto **16a** with the dicationic complexes **2**, **3**, and **5** as catalysts under different reaction conditions. An intriguing feature of this reaction is that both the substrate and Me_3SiCN contain a nitrogen donor and can hence potentially bind to the iron(II) ion (*vide infra*).

The reactions were run with a catalyst loading of 10 mol% and an excess of Me_3SiCN (5 equiv) (Table 4). The

Table 4. Enantioselective Catalytic Addition of Me_3SiCN to Azomethine Imines (Strecker Reaction)[a]

entry	substrate	Ar	catalyst	*t* (h)	yield (%)[b]	ee (%)[c]
1	**16a**	Ph	$2(BF_4)_2$	1.5	99	20
2	**16a**	Ph	$2(SbF_6)_2$	1.5	99	20
3[d]	**16a**	Ph	$2(SbF_6)_2$	7.5	91	22
4	**16a**	Ph	**3**	1.5	95	11
5	**16a**	Ph	**5**	4.5	89	0
6	**16b**	4-MeOPh	$2(SbF_6)_2$	1.5	82	21
7	**16c**	4-CF_3Ph	$2(SbF_6)_2$	1.5	87	17
8[e]	**16a**	Ph	$2(SbF_6)_2$	1.5	49	9
9[f]	**16a**	Ph	$2(SbF_6)_2$	1.5	99	15
10[g]	**16a**	Ph	$2(SbF_6)_2$	1.5	71	8
11	**16a**	Ph	**18**	1.5	91	0

[a]Reaction conditions: substrate (0.17 mmol), catalyst (0.017 mmol), Me_3SiCN (0.86 mmol), CH_2Cl_2 (5 mL), T = −25 °C (unless otherwise stated). [b]Isolated yields. [c]Determined by chiral HPLC. [d]T = −78 °C. [e]Ethyl cyanoformate was used as the cyanide source. [f]1.1 equiv of Me_3SiCN was used. [g]Slow addition of Me_3SiCN (2 μL/min).

DOI: 10.1021/acs.organomet.5b00357
Organometallics XXXX, XXX, XXX−XXX

bis(acetonitrile) derivative $\mathbf{2(BF_4)_2}$ was tested first (entry 1). At −25 °C, the background reaction was much slower than the catalyzed reaction at the same temperature, which typically reaches completion within 1.5 h. Lowering the temperature to −78 °C slowed the reaction down without substantially improving the enantioselectivity (22% ee, entry 3). The counterion (BF_4^-, entry 1; SbF_6^-, entry 2) had no influence on the reaction outcome. The dicarbonyl complex **3** gave lower enantioselectivity (entry 4), whereas the *tert*-butylisonitrile derivative **5** reacted sluggishly and without asymmetric induction (entry 5).

The substrate scope was briefly studied with the best performing catalyst $\mathbf{2(SbF_6)_2}$. An electron-donating group (OMe) on the aryl substituent slightly lowered the yield, but not the enantioselectivity (entry 6), whereas the electron-withdrawing trifluoromethyl group decreased the enantiomeric excess to 17% (entry 7). Alternatively to Me_3SiCN, ethyl cyanoformate was used as cyanide source. Although this has proven to be beneficial in other reports,[24] ethyl cyanoformate lowered both yield and enantioselectivity in combination with $\mathbf{2(SbF_6)_2}$ (entry 8). Also, lowering the excess of TMSCN to 1.1 equiv resulted in lower ee values (entry 9). Slow addition of the cyanide was detrimental to enantioselectivity, too (entry 10).

In an attempt to improve the enantiodiscrimination, we tried to gather insight into the mechanistic features of the reaction. The observation that the addition of trimethylsilyl cyanide to CH_2Cl_2 solutions of azomethine imine **16a** and the catalyst always caused a color change from dark red to light red-orange suggested that Me_3SiCN coordinates to the metal. Therefore, we prepared the corresponding complex by treating the bis(acetonitrile) complex $\mathbf{2(SbF_6)_2}$ with trimethylsilyl cyanide (5 equiv) in dichloromethane (Scheme 6).

Scheme 6. Synthesis of Bis(CNSiMe$_3$) Complex 18

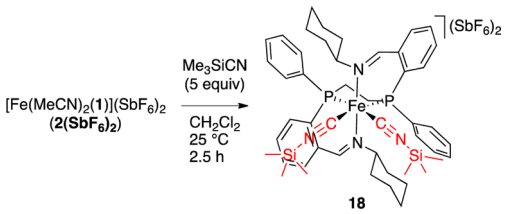

The reaction of **2** with Me_3SiCN, which was accompanied by a similar color change as observed in catalysis, gave an orange solid (**18**) upon precipitation with hexane. The IR spectrum showed two strong bands at 2112 ($CNSiMe)_3$) and 2083 cm^{-1}, which are diagnostic of a isonitrile complex (Fe−$CNSiMe_3$).[25] The assignment based on IR data was confirmed by a broad $^{13}C\{^{31}P,^1H\}$ NMR signal at δ 188.8 for Fe−$CNSiMe_3$.[25a] An X-ray analysis identified complex **18** as Λ-*cis*-α-[Fe($CNSiMe_3$)$_2$-(**1**)](SbF$_6$)$_2$ (see below). Accordingly, the $^{31}P\{^1H\}$ NMR spectrum of **18** shows a singlet at δ 80.7, which indicates that the same configuration is retained in solution. The signal is rather broad (fwhm = 70 Hz), which may hint to facile dissociation of the bulky Me_3SiNC ligand or to a metal-catalyzed isomerization process (see below). The HRMS trace shows a peak at m/z = 698.2507 that corresponds to [Fe(CN)(**1**)]$^+$, which is not surprising given the relative instability of the highly polarized C−Si bond in coordinated trimethylsilyl isocyanide.

The IR data indicate that Me_3SiCN (ν_{NC} ≈ 2191 cm^{-1}) exists in solution in equilibrium with a small amount[26] (ca. 0.2%)[27] of the isonitrile analogue Me_3SiNC (ν_{CN} ≈ 2096 cm^{-1}). Calculations suggest that the isonitrile form (Me_3SiNC) is 3−5 kcal/mol less stable than Me_3SiCN with an activation barrier of 28−30 kcal mol^{-1} for the noncatalyzed interconversion.[28] However, the thermodynamic preference for the cyano form can be reversed by coordination to a transition metal, as documented for titanium[29] and rhenium[30] complexes. The formation of trimethylsilyl isocyanide complexes upon treatment with Me_3SiCN, which has been reported for rhenium(I), is thought to be driven thermodynamically by the stronger net π-acceptor/σ-donor properties of isocyanides as compared to nitriles.[29] The silyl isonitrile complexes are so stable that their formation acts as thermodynamic sinks in the cleavage of the C−C bond of RCN in combination with a silyl ligand on the metal, as reported for rhodium[31] and iron[32] (or of the O−CN bond of cyanates with molybdenum).[33]

X-ray of Λ-*cis*-α-[Fe(CNSiMe$_3$)$_2$(1)](SbF$_6$)$_2$ (18). Orange crystals of **18** were obtained by layering a CH_2Cl_2 solution with hexamethyldisiloxane. The Fe atom lies on a crystallographic two-fold axis and the NPPN ligand adopts the usual Λ-*cis*-α configuration with essentially linear $CNSiMe_3$ ligands (Figure 6). The Fe−$CNSiMe_3$ bond distance in **18** (1.886(7) Å) is very

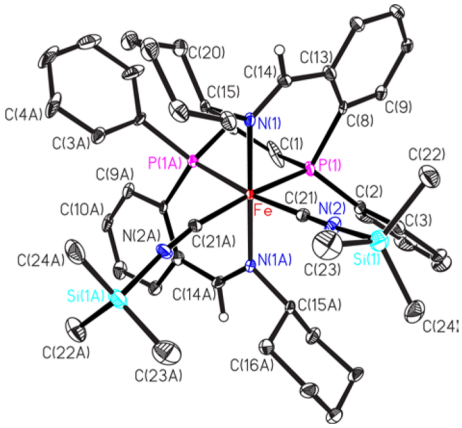

Figure 6. ORTEP drawing of the complex dication of **18** (with ellipsoids at 30% probability).

close to the Fe−CN^{t}Bu separation (1.896(3) Å) in **5**, whereas the P(1)−Fe−C(21) angle (93.8(2)°) suggests that $CNSiMe_3$ is slightly less bulky than CN^{t}Bu (94.80(9)°).

Although N and C atoms can be hardly distinguished by X-ray diffraction, the isonitrile formulation gives a physically more realistic pattern for the thermal parameters of the atoms involved than the alternative Fe−$NCSiMe_3$ description (see Supporting Information).[34] The Fe−C and C−N distances in **18** (Table 5) are similar to those found in [Fe($CNSiMe_3$)-(CO)(Cp)(PPh_3)]$^+$ (1.836(3) and 1.162(4) Å)[25a] and [Fe-($CNSiMe_3$)(CO)$_2$(Cp)]$^+$ (1.862(4) and 1.157(6) Å).[25b] The comparison with $CNSiR_3$ complexes of W,[35] Re,[30] and Rh[31] shows that the C−N distance varies significantly with both the electron density at the metal and the charge of the complex.

Mechanistic Issues. Despite its modest enantioselectivity, the Strecker reaction catalyzed by $\mathbf{2(SbF_6)_2}$ is interesting, as it is the first transition metal-catalyzed cyanide addition onto an azomethine imine. Recently, Wang has reported an organocatalytic, enantioselective version of this reaction that uses a cinchona derivative as hydrogen-bonding catalyst to activate the azomethine imine.[12] In the case of Fe(II)/NPPN, the catalyst may activate either the substrate or Me_3SiCN (or even both).

DOI: 10.1021/acs.organomet.5b00357
Organometallics XXXX, XXX, XXX−XXX

Table 5. Selected Bond Lengths (Å) and Angles (deg) for 18

Fe−P(1)	2.241(2)	Fe−N(1)	2.046(6)
Fe−C(21)	1.886(7)	C(21)−N(1)	1.168(9)
C(21)−Si(1)	1.811(7)		
Fe−C(21)−N(2)	171.3(6)	C(21)−N(2)−Si(1)	174.8(6)
P (1)−Fe−N(1)	92.78(16)	P(1)−Fe−N(1A)	87.71(16)
P(1)−Fe−C(21)	93.8(2)	P(1)−Fe−C(21A)	172.7(2)
N(1)−Fe−C(21)	85.1(3)	N(1)−Fe−C(21A)	94.4(3)
P(1)−Fe−P(1A)	85.17(11)	N(1)−Fe−N(1A)	179.3(3)
C(21)−Fe−C(21A)	88.2(4)		

This is a central issue in view of the importance of metal-catalyzed enantioselective trimethylsilyl cyanide additions in organic synthesis,[36] but also because a thorough understanding of the catalysis intermediates might give insight into the reason for the low enantioselectivity. To that goal, a number of experiments were performed.

When the workup of the reaction mixture was performed under exclusion of water, or when the reaction crude was directly analyzed, the Me_3Si-iminolate derivative **19** (Scheme 7)

Scheme 7. Possible Reaction Pathway for the Strecker Reaction

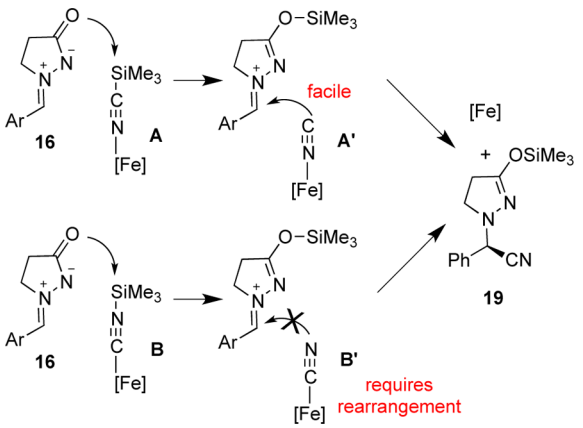

was observed instead of **17**. To check whether the Me_3SiCN/Me_3SiNC isomerization affects the outcome of the Strecker reaction, the bis($CNSiMe_3$) complex **18** was tested as catalyst under the same conditions used with the bis(MeCN) analogue **2**, which gave product **17a** in 91% yield as racemate (Table 4, entry 11).

The observation of **19** suggests that the first reaction step is the transfer of Me_3Si^+ to the oxygen atom the free azomethine imine **16a**, in line with other transition metal-catalyzed additions to azomethine imines, which generally do not involve their coordination to the metal.[37] Me_3Si^+ can arise either from Fe−$NCSiMe_3$ (**A**) or from Fe−$CNSiMe_3$ (**B**), which gives either an isocyano (Fe−NC, **A′**) or a cyano complex (Fe−CN, **B′**) (Scheme 7).[38] The cyano complex **B′** is expected to be less reactive (because more stable) than its isocyano analogue **B**. Also, it contains the CN^- fragment in the wrong orientation for the nucleophilic attack onto the silyl-activated azomethine imine. In turn, the Me_3Si-activated azomethine imine may react with a non-metal-bound trimethylsilyl cyanide molecule in a non-enantioselective fashion. Albeit essentially speculative, such a working hypothesis would accommodate the lack of enantioselectivity of the trimethylsilyl isonitrile complex **18**.

The low enantioselectivity of the Strecker reaction may have a further reason, though. Upon mixing $[Fe(MeCN)_2(\mathbf{1})]SbF_6$ ($\mathbf{2(SbF_6)_2}$), azomethine imine **16a**, and Me_3SiCN (1:1:1 ratio) in CD_2Cl_2 at room temperature, new $^{31}P\{^1H\}$ NMR resonances at δ 88.3, 81.6, and −4.2 in a 0.36:0.55:0.07 ratio appeared within 15 min after mixing the reagents. The chemical shift of the singlet at δ −4.2 is diagnostic of a species with noncoordinated P donors, whereas the signals at δ 88.3 and 81.6 are assigned to the bis(acetonitrile) complex $\mathbf{2(SbF_6)_2}$ and to $[Fe(CNSiMe_3)_2(\mathbf{1})]^{2+}$ (**18**), respectively.[39] The relative intensity of the signal at δ −4.2 increased with time, and, after 12 h, the final ratio of integrals was 0.32:0.44:0.24 for the signal of $\mathbf{2(SbF_6)_2}$, **18**, and the new species at δ −4.2, respectively.

A control experiment showed that the latter species derives from the displacement of ligand **1** from iron by the reaction product. When an excess of independently synthesized, racemic product **17a** (10 equiv) was added to the bis(acetonitrile) derivative $\mathbf{2(SbF_6)_2}$ in CD_2Cl_2, the signal of $\mathbf{2(SbF_6)_2}$ at δ 88.3 disappeared instantaneously, and the singlet at δ −4.2 was the only signal observed. As the free tetradentate ligand **1** gives a $^{31}P\{^1H\}$ NMR singlet at δ −25.2, the structure of the species resonating at δ −4.2 remains elusive, but structures involving dangling phosphines appear probable. As azomethine imine does not displace the NPPN ligand (see above), the product of the Strecker reaction **17a** possibly binds to Fe(II) via the nitrile group. As the phosphine is the stereogenic moiety, its dissociation from iron may account for the low enantioselectivity.

Further experiments were performed with the dicarbonyl complex **3** and with the bis(*tert*-butylisonitrile) derivative **5**, whose reaction with Me_3SiCN (4 equiv) was monitored by $^{31}P\{^1H\}$ NMR spectroscopy. The dicarbonyl complex **3** slowly reacted with Me_3SiCN to give a supposedly Fe−$NCSiMe_3$ intermediate. This then isomerized over time to several species with $^{31}P\{^1H\}$ NMR signals in the δ range 81.5−85.5, which supports the Fe−$CNSiMe_3$ formulation (see Supporting Information, Figure S27). As the MeCN analogue **2** reacts instantaneously to give **18**, and the enantioselective pathway requires the activation of Me_3SiCN by the chiral catalyst, the different substitution lability of these two catalysts may affect the rate of formation of the (yet unknown) active species and explain the lower enantioselectivity of **3** (11% ee, Table 4, entry 4) as compared with **2** (20% ee, entry 1). A further option is the competition of the non-enantioselective reaction, in which the Lewis acidic iron catalyst only serves as a Me_3Si^+ transfer agent, but does not deliver CN^- to the activated substrate.

Finally, the CN^tBu complex **5** failed to react either with Me_3SiCN or with the product of the Strecker reaction **17a**, which suggests that there is no involvement of a metal complex in catalysis, and a slow and non-enantioselective background

DOI: 10.1021/acs.organomet.5b00357
Organometallics XXXX, XXX, XXX−XXX

reaction may account for the slow formation of racemic **17a** observed in catalysis (Table 4, entry 5).

The above experiments suggest at least two reasons for the low enantioselectivity observed in catalysis with the Fe/NPPN catalysts, that is, the isomerization of Me_3SiCN to Me_3SiNC on the iron(II) catalyst and the displacement of the chiral NPPN ligand from the metal by the product of the Strecker reaction **17a**. The facile isomerization of Me_3SiCN to Me_3SiNC, which is triggered by the stability of the resulting isonitrile complex, may hamper cyanide transfer to the substrate. Due to its general nature, this phenomenon is potentially a serious obstacle to the application of late transition metal catalysts to the enantioselective cyanide transfer from silyl cyanides, in contrast to early transition complexes, which successfully catalyze higly enantioselective trimethylsilyl- and hydrocyanation reactions.[40]

Finally, the lability of the NPPN ligand **1** contrasts with the sturdy nature of the closely related macrocycle N_2P_2 ligands that our group reported recently.[6] Albeit disappointing, this is an instructive example of how subtle changes such as moving from an open-chain NPPN to a macrocylic ligand can dramatically affect the stability and catalytic performance of iron(II) catalysts.

CONCLUSIONS

A number of stable, diamagnetic iron(II) complexes have been prepared with a new, *P*-stereogenic open-chain NPPN ligand. The complexes are mostly C_2-symmetric and feature the Λ-*cis*-α geometry. Reactivity studies revealed that these dicationic complexes are highly azaphilic. In view of their readiness to bind nitrogen donors, the new complexes were applied in the first example of transition metal-catalyzed enantioselective nucleophilic addition of trimethylsilyl cyanide to *N*,*N*′-cyclic azomethine imines. However, the enantioselectivity is low, for which at least two possible reasons can be envisaged. First, the isomerization of Me_3SiCN to Me_3SiNC, which is thermodynamically driven by the stability of the resulting isonitrile complexes, produces a Fe−CN complex that can be expected to be an unsuitable CN-transfer reagent for electronic and stereochemical reasons. Second, in the specific case of iron, the coordination of the nitrile-containing product to iron(II) is so strong that it displaces the chiral tetradentate NPPN ligand. This result shows once more that the coordination ability of the chiral ligand is a particularly delicate issue in asymmetric catalysis with iron(II) complexes, as even multidentate ligands are readily displaced despite their substantial chelate effect.

EXPERIMENTAL SECTION

General. All reactions were performed under an argon atmosphere using Schlenk techniques unless otherwise stated. Solvents were of puriss p.a. quality and were distilled under argon atmosphere with standard drying agents (CH_2Cl_2, MeOH, MeCN: CaH_2; Et_2O, toluene: Na/benzophenone; hexane: Na/benzophenone/tetraglyme; EtOH: Na/diethyl phthalate). All solvents were freshly distilled prior to use. NMR spectra were measured on Bruker Avance DPX 300 (^{1}H, 300.1; ^{13}C{^{1}H}, 75.5; ^{31}P{^{1}H}, 121.5), Bruker Avance DPX 400 (^{1}H, 400.1; ^{13}C{^{1}H}, 100.6; ^{31}P{^{1}H}, 162.0) or Bruker Avance DPX 500 (^{1}H, 500.2; ^{13}C{^{1}H,^{31}P}, 125.8; ^{31}P{^{1}H}, 202.5) spectrometers (frequencies in MHz). The internal standard standard was the residual ^{1}H or ^{13}C peak of the deuterated solvent (^{1}H NMR: $CDCl_3$ δ = 7.26; CD_2Cl_2 δ = 5.32; ^{13}C{^{1}H} NMR: $CDCl_3$ δ = 77.16; CD_2Cl_2 δ = 53.84). ^{31}P{^{1}H} NMR spectra are referenced to external 85% H_3PO_4. Thin-layer chromatography (TLC) was performed on Merck silica gel 60 F254 TLC plates; UV light (366 or 254 nm) or $KMnO_4$ was used for detection. Mass spectra were measured by the MS service of the Laboratorium für Organische Chemie (ETH Zürich). The enantiomeric excess was determined by chiral high-performance liquid chromatography (HPLC) using an IA 3 μm column or an AM 5 μm column.

(1*S*,1′*S*)-*N*,*N*′-(((Ethane-1,2-diylbis(phenylphosphinediyl))-bis(2,1-phenylene))bis(methanylylidene))dicyclohexanamine, 1. Cyclohexylamine (0.178 mL, 1.55 mmol, 2.1 equiv) was added to a solution of (1*S*,1′*S*)-2,2′-(ethane-1,2-diylbis(phenylphosphinediyl))-dibenzaldehyde[6a] (336 mg, 0.739 mmol, 1 equiv) in EtOH (7.5 mL). After the mixture was stirred for 24 h at room temperature, the solvent was evaporated, and excess amine was azeotropically removed with toluene to give a white solid. Yield: 460 mg (100%). $[\alpha]_D^{20}$ = −72.0° (*c* = 0.1, CH_2Cl_2). ^{1}H NMR (300 MHz, CD_2Cl_2): δ 9.02 (*s*, 2H, N=C*H*), 7.95−7.89 (*m*, 2H, Ar−*H*), 7.39−7.11 (*m*, 16H, Ar−*H*), 3.21−3.07 (*m*, 2H, N−C*H*), 2.14−2.08 (*m*, 4H, PC*H*H), 1.84−1.10 (*m*, 20H, Cy−*H*). ^{31}P{^{1}H} NMR (122 MHz, CD_2Cl_2): δ −25.2. ^{13}C{^{1}H} NMR (75 MHz, CD_2Cl_2): δ 157.3 (*m*, N=*C*), 141.0 (C_{Ar}), 138.5 (br *m*, C_{Ar}), 134.9 (*m*, C_{Ar}), 133.0 (*t*, $^2J_{P,C}$ = 9.5 Hz, C_{Ar}), 131.7 (C_{Ar}), 130.2 (C_{Ar}), 129.1 (C_{Ar}), 128.9 (C_{Ar}), 128.8 (*t*, $^4J_{P,C}$ = 3.2 Hz, C_{Ar}), 127.7 (C_{Ar}), 70.0 (N−*C*), 34.7 (*d*, $^2J_{P,C}$ = 4.0 Hz, PCH_2), 26.1 (Cy−CH_2), 25.09 (Cy−CH_2), 25.06 (Cy−CH_2), 24.0 (Cy−CH_2), 23.9 (Cy−CH_2). HRMS (MALDI): *m*/*z* calcd for $[M]^+$: 616.3136; found 616.3134. Anal. Calcd for $C_{40}H_{46}N_2P_2$: C, 77.90; H, 7.52; N, 4.54; Found: C, 77.62; H, 7.58; N, 4.53.

Synthesis of (*OC*-6-22)-[Fe(MeCN)$_2$(1)](X)$_2$, 2. $[Fe(OH_2)_6](BF_4)_2$ (319 mg, 0.945 mmol) was added to a solution of **1** (670 mg, 1.09 mmol, 1.15 equiv) in acetonitrile (15 mL), whose color immediately changed from colorless to red. After the mixture was stirred for 3 h, the solvent was removed under reduced pressure. Red crystals were obtained by dissolving the crude in acetonitrile and layering with diethyl ether. The SbF_6^- salt, obtained from $[Fe(MeCN)_6](SbF_6)_2$ instead of $[Fe(OH_2)_6](BF_4)_2$, showed essentially the same spectroscopic data, but improved elemental analytic data, possibly due to better combustion behavior. Yield: 660 mg (75%). ^{1}H NMR (300 MHz, CD_2Cl_2): δ 8.17 (*s*, 2H, N=C*H*), 7.80−7.58 (*m*, 6H, Ar-*H*), 7.56−7.43 (*m*, 8H, Ar-*H*), 7.33−7.21 (*m*, 4H, Ar−*H*), 3.56−3.47 (*m*, 2H, N−C*H*), 2.86 (*dd*, $^2J_{P,H}$ = 29.0 Hz, $^2J_{H,H'}$ = 9.0 Hz, 2H, PC*H*H), 2.45 (*s*, 6H, NCCH_3), 2.28−2.11 (*m*, 4H, PC*H*H and Cy−*H*), 1.89−1.79 (*m*, 2H, Cy−*H*), 1.69−1.51 (*m*, 4H, Cy−*H*), 1.38−1.02 (*m*, 10H, Cy−*H*), 0.87−0.66 (*m*, 2H, Cy−*H*). ^{31}P{^{1}H} NMR (122 MHz, CD_2Cl_2): δ 88.3. ^{13}C{^{1}H} NMR (101 MHz, CD_2Cl_2): δ 175.4 (N=*C*), 137.7 (*m*, C_{Ar}), 137.1 (*m*, C_{Ar}), 134.9 (*m*, C_{Ar}), 133.6 (C_{Ar}), 132.6 (C_{Ar}), 132.2 (*t*, $^3J_{P,C}$ = 4.3 Hz, C_{Ar}), 132.0 (C_{Ar}), 131.3 (br *m*, C_{Ar}), 130.2 (*t*, $^3J_{P,C}$ = 4.9 Hz, C_{Ar}), 74.0 (N−*C*), 36.1 (PCH_2), 34.0 (Cy−CH_2), 26.5 (Cy−CH_2), 26.3 (Cy−CH_2), 26.0 (Cy−CH_2), 25.8 (Cy−CH_2), 4.6 (CH_3). The quaternary carbon atom of the acetonitrile and one quaternary aromatic carbon atom are not resolved. HRMS (MALDI): *m*/*z* calcd for $[M - 2MeCN]^+$: 672.2486, found 672.2480; calcd for $[M - 2MeCN + F]^+$): 691.2470, found 691.2467. IR (KBr pellet, cm^{-1}): 2315 ($NCCH_3$), 2279 ($NCCH_3$). Anal. Calcd for $C_{44}H_{52}FeN_4P_2B_2F_8$ (BF_4^- salt): C, 56.93; H, 5.65; N, 6.04. Found: C, 56.76; H, 5.70; N, 7.03. Anal. Calcd for $C_{44}H_{52}FeN_4P_2Sb_2F_{12}$ (SbF_6^- salt): C, 43.10; H, 4.27; N, 4.57. Found: C, 43.11; H, 4.28; N, 4.51.

Synthesis of (*OC*-6-33)-[Fe(CO)$_2$(1)](BF$_4$)$_2$, 3. Complex **2**$(BF_4)_2$ (300 mg, 0.323 mmol) was dissolved in acetone (16 mL) in a 50 mL Young Schlenk flask. The argon atmosphere was then removed and replaced by CO (2.25 bar), the solution was stirred for 20 min, and the volatiles were removed under reduced pressure. The procedure was repeated until no further color change (red to yellow) was observed (3−4 times). Then, the crude was redissolved in dichloromethane (10 mL) and layered with diethyl ether (70 mL) under CO atmosphere (1.2 bar). After 2 days, the mother liquor was decanted, and the product was dried to give yellow-greenish crystals. Yield: 260 mg (89%). ^{1}H NMR (500 MHz, CD_2Cl_2): δ 8.23 (*s*, 2H, N=C*H*), 8.00−7.91 (*m*, 4H, Ar−*H*), 7.88−7.83 (*m*, 2H, Ar−*H*), 7.82−7.69 (*m*, 10H, Ar−*H*), 7.63−7.55 (*m*, 2H, Ar−*H*), 3.11 (*dd*, $^2J_{P,H}$ = 43.9 Hz, $^2J_{H,H'}$ = 9.2 Hz, 2H, PC*H*H), 2.77 (*d*, $^3J_{H,H'}$ = 11.2 Hz, 2H, N−C*H*), 2.68 (*d*, $^2J_{H,H'}$ = 9.2 Hz, 2H, PC*H*H), 2.43 (*d*, $^3J_{H,H'}$ = 10.8 Hz, 2H, Cy−H_{eq}), 1.96 (*d*, $^3J_{H,H'}$ = 9.2 Hz, 2H, Cy−H_{eq}), 1.57−1.45 (*m*, 6H, Cy−*H*),

DOI: 10.1021/acs.organomet.5b00357
Organometallics XXXX, XXX, XXX−XXX

1.30−1.19 (*m*, 4H, Cy−*H*), 1.12−1.02 (*m*, 2H, Cy−*H*), 0.74 (*d*, $^3J_{H,H'}$ = 11.3 Hz, 2H, Cy−*H*), 0.29 (*q*, $^3J_{H,H'}$ = 13.2 Hz, 2H, Cy−*H*). $^{31}P\{^1H\}$ NMR (122 MHz, CD_2Cl_2): δ 79.6. $^{13}C\{^{31}P,^1H\}$ NMR (126 MHz, CD_2Cl_2): δ 207.8 (CO), 176.7 (*C*═N), 141.9 (C_{Ar}), 137.1 (C_{Ar}), 135.9 (C_{Ar}), 135.5 (C_{Ar}), 134.5 (C_{Ar}), 134.0 (C_{Ar}), 133.5 (C_{Ar}), 131.5 (C_{Ar}), 126.6 (C_{Ar}), 120.0 (C_{Ar}), 84.5 (N−*C*), 35.6 (PCH_2), 34.9 (Cy−CH_2), 26.8 (Cy−CH_2), 26.7 (Cy−CH_2), 26.5 (Cy−CH_2), 25.4 (Cy−CH_2). HRMS (MALDI): *m*/*z* calcd for $[M + H]^+$: 729.2462, found 729.2453. IR (KBr pellet, cm^{-1}): 2072 (CO), 2028 (CO). Anal. Calcd for $C_{42}H_{46}B_2F_8FeN_2P_2O_2 \cdot CH_2Cl_2$: C, 52.32; H, 4.90; N, 2.84. Found: C, 52.34; H, 4.96; N, 2.80. One equivalent of dichloromethane is incorporated in the crystals obtained by the method described above. For a powdered, dried sample, the following analytical data were collected. Anal. Calcd for $C_{42}H_{46}B_2F_8FeN_2P_2O_2$: C, 55.91; H, 5.14; N, 3.10. Found: C, 56.14; H, 5.37; N, 2.88.

Synthesis of [FeBr(CO)(1)](BPh$_4$), 4. KBr (64 mg, 0.54 mmol, 2 equiv) and **2**$(BF_4)_2$ (249.5 mg, 0.27 mmol) were dried under vacuum for 15 min. Acetone (15 mL) was added, and the mixture was gently heated until all solids dissolved. The argon atmosphere was then removed and replaced with CO (2.25 bar). The mixture was stirred for 2 days (whereby the CO atmosphere has been replaced 4 times), followed by removal of volatiles under reduced pressure. Then, the crude was dissolved in MeOH (7 mL), filtered, and sodium tetraphenylborate (92 mg, 0.27 mmol, 1 equiv) in MeOH (1 mL) was added to the filtered solution. The resulting precipitate was filtered off to give an orange powder. Yield: 167 mg (57%). ^1H NMR (400 MHz, CD_2Cl_2): δ 9.07−9.04 (*m*, 0.2H, N═C*H*), 8.83−8.77 (*m*, 0.4H, N═C*H*), 7.95−7.91 (*m*, 1.5H, N═C*H*), 7.86−7.35 (*m*, 18H, Ar−*H*), 7.34−7.28 (*m*, 8H, BPh_4), 7.00 (*t*, $^3J_{H,H'}$ = 7.4 Hz, 8H, BPh_4), 6.87 (*t*, $^3J_{H,H'}$ = 7.2 Hz, 4H, BPh_4), 4.23 (*t*, $^3J_{H,H'}$ = 10.7 Hz, 2H, NC*H*), 3.6−0.6 (*m*, 24H, $H_{aliphatic}$). $^{31}P\{^1H\}$ NMR (121 MHz, CD_2Cl_2): δ 93.7 (*d*, $^2J_{P,P'}$ = 49.6 Hz), 91.7 (*d*, $^2J_{P,P'}$ = 35.1 Hz), 86.8 (*d*, $^2J_{P,P}$ = 34.9 Hz), 85.0 (*d*, $^2J_{P,P'}$ = 38.0 Hz), 73.8 (*d*, $^2J_{P,P'}$ = 38.1 Hz), 68.6 (*d*, $^2J_{P,P'}$ = 49.6 Hz). See Results and Discussion for signal attribution. IR (ATR, in cm^{-1}): υ = 1986 (CO), 1961 (CO). HRMS (MALDI): *m*/*z* calcd for $[M-CO]^+$: 751.1669, found 751.1663. Anal. Calcd for $C_{65}H_{66}BBrFeN_2OP_2$: C, 70.99; H, 6.05; N, 2.55. Found: C, 70.73; H, 6.02; N, 2.48.

Synthesis of (*OC*-6-33)-[Fe(CN^{t}Bu)$_2$(1)](BF$_4$)$_2$, 5. *tert*-Butylisocyanide (20 μL, 0.181 mmol, 4 equiv) was added to a solution of **2**$(BF_4)_2$ (42 mg, 0.045 mmol) in dichloromethane (3 mL). After being stirred for 2 h, the solution was concentrated to 1 mL and layered with hexane (11 mL) to give orange crystals. Yield: 40 mg (87%). ^1H NMR (300 MHz, CD_2Cl_2): δ 8.07 (*s*, 2H, N═C*H*), 7.90−7.80 (*m*, 2H, Ar−*H*), 7.75−7.65 (*m*, 6H, Ar−*H*), 7.63−7.47 (*m*, 10H, Ar−*H*), 2.96 (*dd*, $^2J_{P,H}$ = 36.1 Hz, $^2J_{H,H'}$ = 8.7 Hz, 2H, PC*H*H), 2.70 (*t*, $^3J_{H,H'}$ = 11.0 Hz, 2H, N−C*H*), 2.60 (*d*, $^3J_{H,H'}$ = 11.4 Hz, 2H, Cy−H_{eq}), 2.36 (*d*, $^2J_{H,H'}$ = 8.7 Hz, 2H, PC*H*H), 1.94 (*d*, $^3J_{H,H'}$ = 12.4 Hz, 2H, Cy−H_{eq}), 1.51 (*s*, 18H, CNC(CH_3)$_3$), 1.46−1.00 (*m*, 12H, Cy−*H*), 0.41−0.21 (*m*, 4H, Cy−*H*). $^{31}P\{^1H\}$ NMR (122 MHz, CD_2Cl_2): δ 82.4. $^{13}C\{^1H\}$ NMR (101 MHz, CD_2Cl_2): δ 175.4 (N═*C*), 139.7 (*m*, C_{Ar}), 137.0 (*m*, C_{Ar}), 135.8 (*m*, C_{Ar}), 134.4 (C_{Ar}), 133.6 (C_{Ar}), 133.1 (C_{Ar}), 133.0 (C_{Ar}), 130.5 (*m*, C_{Ar}), 122.1 (br *m*, C_{Ar}), 81.1 (N−*C*), 60.9 (*C*(CH_3)$_3$), 35.7 (PCH_2), 34.0 (2C, Cy−CH_2), 30.7 (C(CH_3)$_3$), 26.8 (2C, Cy−CH_2), 25.4 (Cy−CH_2). The quaternary carbon atom of the isonitrile and one quaternary aromatic carbon are not resolved. HRMS (MALDI): *m*/*z* calcd for $[M]^+$: 838.3956, found 838.3949. IR (ATR, cm^{-1}): 2162 (^{t}BuNC), 2143 (^{t}BuNC). Anal. Calcd for $C_{50}H_{64}B_2F_8FeN_4P_2$: C, 59.31; H, 6.37; N, 5.53. Found: C, 59.14; H, 6.27; N, 5.32.

Synthesis of (*OC*-6-22)-[Fe(CNSiMe$_3$)$_2$(1)](SbF$_6$)$_2$, 18. Trimethylsilyl cyanide (53 μL, 0.4 mmol, 5 equiv) was added to a solution of **2**$(SbF_6)_2$ (97 mg, 0.079 mmol) in dichloromethane (4 mL), and stirred for 5 h, after which hexane was added to precipitate the product. Yield: 76 mg (71%). ^1H NMR (300 MHz, CD_2Cl_2): δ 8.00 (*s*, 2H, N═C*H*), 7.87−7.33 (*m*, 18H, Ar−*H*), 3.20−2.64 (*m*, 6H, PCH_2 and N−C*H*), 2.36−2.18 (*m*, 2H, Cy−H_{eq}), 1.95−1.75 (*m*, 2H, Cy−H_{eq}), 1.60−1.34 (*m*, 4H, Cy−H_{eq}), 1.33−0.82 (*m*, 1H, Cy−*H*), 0.37 (*s*, 18H, Si(CH_3)$_3$), 0.26−0.08 (*m*, 2H, Cy−*H*). $^{31}P\{^1H\}$ NMR (122 MHz, CD_2Cl_2): δ 80.7. For the BF_4^- salt, a shift of δ 82.9 is observed. $^{13}C\{^{31}P,^1H\}$ NMR (126 MHz, CD_2Cl_2): δ 188.8 (*C*NSi(CH_3)$_3$), 174.5 (*C*═N), 139.5 (C_{Ar}), 136.8 (C_{Ar}), 136.0 (C_{Ar}), 134.4 (C_{Ar}), 133.8 (C_{Ar}), 133.2 (C_{Ar}), 133.0 (C_{Ar}), 130.6 (C_{Ar}), 130.0 (C_{Ar}), 122.1 (C_{Ar}), 81.5 (N−C_{Cy}), 36.0 (PCH_2), 34.1 (Cy−CH_2), 27.2 (Cy−CH_2), 26.8 (Cy−CH_2), 26.6 (Cy−CH_2), 25.5 (Cy−CH_2), 0.1 (Si(CH_3)$_3$). HRMS (MALDI): *m*/*z* calcd for $[Fe(CN)(\mathbf{1})]^+$: 698.2516, found 698.2507. IR (ATR, cm^{-1}): 2112 (*C*NSi(CH_3)$_3$), 2083 (*C*NSi(CH_3)$_3$). Anal. Calcd for $C_{48}H_{64}F_{12}FeN_4P_2Si_2Sb_2$: C, 42.94; H, 4.80; N, 4.17. Found: C, 43.15; H, 4.91; N, 4.23.

General Procedure for the Synthesis of Enantioenriched 2-(3-Oxopyrazolidin-1-yl)-2-arylacetonitriles. Catalyst (0.017 mmol, 10 mol%) was dissolved in dichloromethane (5 mL), and the appropriate 2-arylidene-5-oxopyrazolidin-2-ium-1-ide (**16a**−**16c**, 0.17 mmol) was added to the reaction solution, which was cooled to −25 °C. Me_3SiCN (115 μL, 0.86 mmol, 5 equiv) was added in one portion and the mixture was stirred at −25 °C. Reaction progress was checked by TLC (10% MeOH in dichloromethane). After the reaction was complete, the reaction mixture was filtered through a pad of silica gel, which was washed thoroughly with ethyl acetate. Evaporation of the solvent under reduced pressure gave products **17a**−**17c** as off-white solids. For characterization details, see Supporting Information.

■ ASSOCIATED CONTENT

Ⓢ Supporting Information

^1H, ^{31}P, and ^{13}C NMR spectra, details of X-ray structures, substrate synthesis, and product characterization data. The Supporting Information is available free of charge on the ACS Publications website at DOI: 10.1021/acs.organomet.5b00357.

■ AUTHOR INFORMATION

Corresponding Author

*E-mail: mezzetti@inorg.chem.ethz.ch.

Notes

The authors declare no competing financial interest.

■ ACKNOWLEDGMENTS

This work was supported by the Swiss National Foundation (SNF), Grant No. 200020_146881.

■ REFERENCES

(1) For selected reviews, see: (a) Sherry, B. D.; Fürstner, A. *Acc. Chem. Res.* **2008**, *41*, 1500−1511. (b) Enthaler, S.; Junge, K.; Beller, M. *Angew. Chem., Int. Ed.* **2008**, *47*, 3317−3321. (c) Morris, R. H. *Chem. Soc. Rev.* **2009**, *38*, 2282−2291. (d) Gopalaiah, K. *Chem. Rev.* **2013**, *113*, 3248−3296. (e) Bauer, I.; Knölker, H.-J. *Chem. Rev.* **2015**, *115*, 3170−3387.

(2) Bertini, I.; Gray, H. B.; Lippard, S. J.; Valentine, J. S. *Bioinorganic Chemistry*; University Science Books: Mill Valley, CA, 1994.

(3) (a) Bart, S.; Lobkovsky, E.; Chirik, P. J. *J. Am. Chem. Soc.* **2004**, *126*, 13794−13807. (b) Tondreau, A. M.; Atienza, C. C. H.; Weller, K. J.; Nye, S. A.; Lewis, K. M.; Delis, J. G. P.; Chirik, P. J. *Science* **2012**, *335*, 567−570. (c) Langer, R.; Leitus, G.; Ben-David, Y.; Milstein, D. *Angew. Chem., Int. Ed.* **2011**, *50*, 2120−2124. (d) Langer, R.; Iron, M. A.; Konstantinovski, L.; Diskin-Posner, Y.; Leitus, G.; Ben-David, Y.; Milstein, D. *Chem.—Eur. J.* **2012**, *18*, 7196−7209. (e) Langer, R.; Diskin-Posner, Y.; Leitus, G.; Shimon, L.; Ben-David, Y.; Milstein, D. *Angew. Chem., Int. Ed.* **2011**, *50*, 9948−9952. (f) Zell, T.; Butschke, B.; Ben-David, Y.; Milstein, D. *Chem.—Eur. J.* **2013**, *19*, 8068−8072. (g) Lagaditis, P. O.; Sues, P. E.; Sonnenberg, J. F.; Wan, K. Y.; Lough, A. J.; Morris, R. H. *J. Am. Chem. Soc.* **2014**, *136*, 1367−1380.

(4) (a) Chen, M. S.; White, M. C. *Science* **2007**, *318*, 783−787. (b) Chen, M. S.; White, M. C. *Science* **2010**, *327*, 566−571. (c) Bigi, M. A.; Reed, S. A.; White, M. C. *Nat. Chem.* **2011**, *3*, 216−222. (d) Bigi, M. A.; Liu, P.; Zou, L.; Houk, K. N.; White, M. C. *Synlett* **2012**, *23*, 2768−2772. (e) Bigi, M. A.; Reed, S. A.; White, M. C. *J. Am. Chem. Soc.* **2012**, *134*, 9721−9726. (f) Gormisky, P. E.; White, M. C. *J. Am. Chem. Soc.* **2013**, *135*, 14052−14055. (g) Zhou, S.; Fleischer, S.; Junge, K.; Das, S.; Addis, D.; Beller, M. *Angew. Chem., Int. Ed.* **2010**,

DOI: 10.1021/acs.organomet.5b00357
Organometallics XXXX, XXX, XXX−XXX

49, 8121−8125. (h) Wienhöfer, G.; Sorribes, I.; Boddien, A.; Westerhaus, F.; Junge, K.; Junge, H.; Llusar, R.; Beller, M. *J. Am. Chem. Soc.* **2011**, *133*, 12875−12879. (i) Wienhöfer, G.; Westerhaus, F.; Jagadeesh, R.; Junge, K.; Junge, H.; Beller, M. *Chem. Commun.* **2012**, *48*, 4827−4829. (j) Ziebart, C.; Federsel, C.; Pazhamalai, A.; Jackstell, R.; Baumann, W.; Spannenberg, A.; Beller, M. *J. Am. Chem. Soc.* **2012**, *134*, 20701−20704. (k) Wienhöfer, G.; Westerhaus, F.; Junge, K.; Ludwig, R.; Beller, M. *Chem.—Eur. J.* **2013**, *19*, 7701−7707. (l) Wienhöfer, G.; Westerhaus, F.; Junge, K.; Beller, M. *J. Organomet. Chem.* **2013**, *744*, 156−159. (m) Buchard, A.; Heuclin, H.; Auffrant, A.; Le Goff, X. F.; Le Floch, P. *Dalton Trans.* **2009**, 1659−1667. (n) Sui-Seng, C.; Freutel, F.; Lough, A. J.; Morris, R. H. *Angew. Chem., Int. Ed.* **2008**, *47*, 940−943. (o) Mikhailine, A. A.; Lough, A. J.; Morris, R. H. *J. Am. Chem. Soc.* **2009**, *131*, 1394−1395. (p) Meyer, N.; Lough, A. L.; Morris, R. H. *Chem.—Eur. J.* **2009**, *15*, 5605−5610. (q) Lagaditis, P. O.; Mikhailine, A. A.; Lough, A. J.; Morris, R. H. *Inorg. Chem.* **2010**, *49*, 1094−1102. (r) Lagaditis, P. O.; Lough, A. J.; Morris, R. H. *Inorg. Chem.* **2010**, *49*, 10057−10066. (s) Mikhailine, A. A.; Morris, R. H. *Inorg. Chem.* **2010**, *49*, 11039−11044. (t) Sonnenberg, J. F.; Coombs, N.; Dube, P. A.; Morris, R. H. *J. Am. Chem. Soc.* **2012**, *134*, 5893−5899. (u) Mikhailine, A. A.; Maishan, M. I.; Lough, A. J.; Morris, R. H. *J. Am. Chem. Soc.* **2012**, *134*, 12266−12280. (v) Prokopchuk, D. E.; Morris, R. H. *Organometallics* **2012**, *31*, 7375−7385. (w) Zuo, W.; Lough, A. J.; Li, Y. F.; Morris, R. H. *Science* **2013**, *342*, 1080−1083. (x) Zuo, W.; Tauer, S.; Prokopchuk, D. E.; Morris, R. H. *Organometallics* **2014**, *33*, 5791−5801. (y) Hoyt, J. M.; Shevlin, M.; Margulieux, G. M.; Krska, S. W.; Tudge, M. T.; Chirik, P. J. *Organometallics* **2014**, *33*, 5781−5790.

(5) Cabbiness, D. K.; Margerum, D. W. *J. Am. Chem. Soc.* **1969**, *91*, 6540−6541.

(6) (a) Bigler, R.; Otth, E.; Mezzetti, A. *Organometallics* **2014**, *33*, 4086−4099. (b) Bigler, R.; Mezzetti, A. *Org. Lett.* **2014**, *16*, 6460−6463. (c) Bigler, R.; Huber, R.; Mezzetti, A. *Angew. Chem., Int. Ed.* **2015**, *17*, 5171−5174.

(7) (a) Chen, J. S.; Chen, L. L.; Xing, Y.; Chen, G.; Shen, W. Y.; Dong, Z. R.; Li, Y. Y.; Gao, J. X. *Acta Chim. Sin.* **2004**, *62*, 1745−1750. (b) Yu, S. L.; Shen, W. Y.; Li, Y. Y.; Dong, Z. R.; Xu, Y. Q.; Li, Q.; Zhang, J. N.; Gao, J. X. *Adv. Synth. Catal.* **2012**, *354*, 818−822. (c) Li, Y.; Yu, S.; Wu, X.; Xiao, J.; Shen, W.; Dong, Z.; Gao, J. *J. Am. Chem. Soc.* **2014**, *136*, 4031−4039.

(8) Parr, R. G.; Pearson, R. G. *J. Am. Chem. Soc.* **1983**, *105*, 7512−7516.

(9) (a) Mezzetti, A. *Dalton Trans.* **2010**, *39*, 7851−7869. (b) Schotes, C.; Mezzetti, A. *J. Am. Chem. Soc.* **2010**, *132*, 3652−3653. (c) Schotes, C.; Mezzetti, A. *Angew. Chem., Int. Ed.* **2011**, *50*, 3072−3074. (d) Schotes, C.; Althaus, M.; Aardoom, R.; Mezzetti, A. *J. Am. Chem. Soc.* **2012**, *134*, 1331−1343. (e) Egloff, J.; Ranocchiari, M.; Schira, A.; Schotes, C.; Mezzetti, A. *Organometallics* **2013**, *32*, 4690−4701.

(10) (a) Stanley, L. M.; Sibi, M. P. *Chem. Rev.* **2008**, *108*, 2887−2902. (b) Milosevic, S.; Togni, A. *J. Org. Chem.* **2013**, *78*, 9638−9646. (c) Guo, H.; Liu, H.; Zhu, F. L.; Na, R.; Jiang, H.; Wu, Y.; Zhang, L.; Li, Z.; Yu, H.; Wang, B.; Xiao, Y.; Hu, X. P.; Wang, M. *Angew. Chem., Int. Ed.* **2013**, *52*, 12641−12645. (d) Tong, M. C.; Chen, X.; Tao, H. Y.; Wang, C. J. *Angew. Chem., Int. Ed.* **2013**, *52*, 12377−12380. (e) Yamashita, Y.; Kobayashi, S. *Chem.—Eur. J.* **2013**, *19*, 9420−9427. (f) Li, J.; Lian, X.; Liu, X.; Lin, L.; Feng, X. *Chem.—Eur. J.* **2013**, *19*, 5134−5140. (g) Tšupova, S.; Mäeorg, U. *Heterocycles* **2014**, *88*, 129−173.

(11) (a) Burger, K.; Thenn, W.; Schickaneder, H. *Chem. Ber.* **1975**, *108*, 1468−1474. (b) Kawai, H.; Kusuda, A.; Nakamura, S.; Shiro, M.; Shibata, N. *Angew. Chem., Int. Ed.* **2009**, *48*, 6324−6327. (c) Okusu, S.; Kawai, H.; Xu, X. H.; Tokunaga, E.; Shibata, N. *J. Fluorine Chem.* **2012**, *143*, 216−219. (d) Shintani, R.; Soh, Y. T.; Hayashi, T. *Org. Lett.* **2010**, *12*, 4106−4109. (e) Hashimoto, T.; Kimura, H.; Kawamata, Y.; Maruoka, K. *Nat. Chem.* **2011**, *3*, 642−646. (f) Hashimoto, T.; Omote, M.; Maruoka, K. *Angew. Chem., Int. Ed.* **2011**, *50*, 8952−8955. (g) Hashimoto, T.; Kimura, H.; Kawamata, Y.; Maruoka, K. *Angew. Chem., Int. Ed.* **2012**, *51*, 7279−7281.

(12) (a) Li, N.; Liu, Z.; Huang, X.; Zhang, J.; Chen, X.; Wang, Y.; Wang, X. *RSC Adv.* **2013**, *3*, 9154−9157. (b) For an organocatalytic Strecker reaction with Et_2AlCN as nucleophile, see: Kaur, P.; Pindi, S.; Wever, W.; Rajale, T.; Li, G. G. *J. Org. Chem.* **2010**, *75*, 5144−5150.

(13) $[Fe(MeCN)_6](SbF_6)_2$ was prepared by double chloride abstraction from anhydrous $FeCl_2$ using $AgSbF_6$ in acetonitrile and stored in a glovebox.

(14) Marcó, A.; Compañó, R.; Rubio, R.; Casals, I. *Microchim. Acta* **2003**, *142*, 13−19.

(15) Garrou, P. E. *Inorg. Chem.* **1975**, *14*, 1435−1439.

(16) (a) In the case of a *trans P*−M−N=C*H* arrangement, the $^4J_{P,H}$ is large enough to split the imine proton into a doublet and to generate cross peaks in the P,H 2D NMR spectrum.. (b) Schotes, C.; Ranocchiari, M. M.; Mezzetti, A. *Organometallics* **2011**, *30*, 3596−3602.

(17) Yoon, T. P.; Jacobsen, E. N. *Science* **2003**, *299*, 1691−1693.

(18) (a) Li, S. L.; Mak, T. C. W.; Zhang, Z. Z. *J. Chem. Soc., Dalton Trans.* **1996**, 3475−3483. (b) Burrows, A. D.; Dodds, D.; Kirk, A. S.; Lowe, J. P.; Mahon, M. F.; Warren, J. E.; Whittlesey, M. K. *Dalton Trans.* **2007**, 570−580.

(19) Typical values are around 2000 cm^{-1}; see ref 4p and the following: (a) Henry, R. M.; Shoemaker, R. K.; Newell, R. H.; Jacobsen, G. M.; DuBois, D. L.; Rakowski DuBois, M. *Organometallics* **2005**, *24*, 2481−2491. (b) Kohl, S. W.; Heinemann, F. W.; Hummert, M.; Bauer, W.; Grohmann, A. *Chem.—Eur. J.* **2006**, *12*, 4313−4320. (c) Benito-Garagorri, D.; Wiedermann, J.; Pollak, M.; Mereiter, K.; Kirchner, K. *Organometallics* **2007**, *26*, 217−222.

(20) Benito-Garagorri, D.; Alves, L. G.; Veiros, L. F.; Standfest-Hauser, C. M.; Tanaka, S.; Mereiter, K.; Kirchner, K. *Organometallics* **2010**, *29*, 4932−4942.

(21) Pidcock, A.; Richards, R. E.; Venanzi, L. M. *J. Chem. Soc. A* **1966**, 1707−1710.

(22) For two reports on the *trans*-influence of isonitriles in platinum complexes, see: (a) Jovanović, B.; Manojlović, M. J. *J. Chem. Soc., Dalton Trans: Inorg. Chem.* **1972**, *11*, 1176−1178. (b) Ros, R.; Renaud, J.; Roulet, R. *J. Organomet. Chem.* **1976**, *104*, 271−279.

(23) Johnson, L. K.; Killian, C. M.; Brookhart, M. *J. Am. Chem. Soc.* **1995**, *117*, 6414−6415.

(24) (a) Saravasan, S.; Khan, N.; Bera, P. K.; Kureshi, R. I.; Abdi, S. H. R.; Kumar, P.; Bajaj, H. C. *ChemCatChem* **2013**, *6*, 1374−1385. (b) Kumar, P.; Saravanan, S.; Khan, N.; Hussain, F.; Singh, S. *Eur. J. Inorg. Chem.* **2014**, *29*, 5077−5083.

(25) (a) Nakazawa, H.; Itazaki, M.; Owaribe, M. *Acta Crystallogr.* **2005**, *E61*, m1172−m1173. (b) Nakazawa, H.; Itazaki, M.; Owaribe, M. *Acta Crystallogr.* **2005**, *E61*, m1173−m1174.

(26) Bither, T. A.; Knoth, W. H.; Lindsey, R. V.; Sharkey, W. H. *J. Am. Chem. Soc.* **1958**, *80*, 4151−4153.

(27) (a) Booth, M. R.; Frankiss, S. G. *Chem. Commun.* **1968**, 1347−1348. (b) Seckar, J. A.; Thayer, J. S. *Inorg. Chem.* **1976**, *15*, 501−504.

(28) (a) Tao, J. C.; Guo, Y.; Li, S. H. *J. Mol. Struct.: THEOCHEM* **2009**, *899*, 61−70. (b) Wang, J. Y.; Cai, D. L.; Zhang, M.; Wang, M. *J. Organomet. Chem.* **2013**, *724*, 117−128.

(29) Bochmann, M.; Wilson, L. M.; Hursthouse, M. B.; Motevalli, M. *Organometallics* **1988**, *7*, 1148−1154.

(30) Guedes da Silva, M. F.; Lemos, M. A. N. D. A.; Frausto da Silva, J. J. R.; Pombeiro, A. J. L.; Pellinghelli, M. A.; Tiripicchio, A. *Dalton Trans.* **2000**, 373−380.

(31) Taw, F. L.; White, P. S.; Bergman, R. G.; Brookhart, M. *J. Am. Chem. Soc.* **2002**, *124*, 4192−4193.

(32) Nakazawa, H.; Kawasaki, T.; Miyoshi, K.; Suresh, C. H.; Koga, N. *Organometallics* **2004**, *23*, 117−126.

(33) Fukumoto, K.; Dahy, A. A.; Oya, T.; Hayasaka, K.; Itazaki, M.; Koga, N.; Nakazawa, H. *Organometallics* **2012**, *31*, 787−790.

(34) (a) On the basis of the same criterion and the IR data, the structure of $[Ni(NCSiMe_3)(PPh_3)_3]$, which was claimed to be a Ni−$NCSiMe_3$ complex, may deserve reexamination. (b) Wilhelm, D.; Hoffmann, T.; Wenschuh, E.; Reck, G.; Winter, G. *Z. Anorg. Allg. Chem.* **1993**, *619*, 1801−1805.

DOI: 10.1021/acs.organomet.5b00357
Organometallics XXXX, XXX, XXX−XXX

(35) Suzuki, E-; Komuro, T.; Kanno, Y.; Okazaki, Y.; Tobita, H. *Organometallics* **2018**, *29*, 1838−1848.
(36) Weber, W. P. *Silicon Reagents for Organic Synthesis*; Springer Verlag: Berlin, 1983; pp 6−20.
(37) For instance, the rhodium(I)-catalyzed phenylation of azomethine imines with $NaBPh_4$ is thought to involve the formation of a rhodium−phenyl intermediate.[11d] Analogously, a Cu(box)−acetylide complex transfers RCC^- to *C,N*-cyclic azomethine imines in the presence of a Brønsted acid cocatalyst in excellent yield and with high enantioselectivity.[11f]
(38) A similar ambiguity has been discussed for the oxidative addition of silyl cyanides to rhodium(II) porphyrins: Chan, K. S.; Zhang, L.; Fung, C. W. *Organometallics* **2004**, *23*, 6097−6098.
(39) In this experiment, the $^{31}P\{^1H\}$ NMR signal of **18** (δ 81.6) is slightly shifted toward that of $\mathbf{2(SbF_6)_2}$ as compared to the chemical shift of isolated **18** (δ 80.7), which we tentatively attribute to chemical exchange between **18** and $\mathbf{2(SbF_6)_2}$. Accordingly, when Me_3SiCN (1 equiv) is added to $\mathbf{2(SbF_6)_2}$ in CD_2Cl_2 at −78 °C, the $^{31}P\{^1H\}$ NMR spectrum of the reaction mixture shows singlets at δ 88.2 and 80.8, which are assigned to $\mathbf{2(SbF_6)_2}$ and **18**, respectively.
(40) Brunel, J. M.; Holmes, I. P. *Angew. Chem., Int. Ed.* **2004**, *43*, 2752−2778.

DOI: 10.1021/acs.organomet.5b00357
Organometallics XXXX, XXX, XXX−XXX